

# Optically pumped quantum-dot Cd(Zn)Se/ZnSe laser and microchip converter for yellow–green spectral region

E.V. Lutsenko, A.G. Voinilovich, N.V. Rzhetskii, V.N. Pavlovskii, G.P. Yablonskii, S.V. Sorokin, S.V. Gronin, I.V. Sedova, P.S. Kop'ev, S.V. Ivanov, M. Alanzi, A. Hamidalddin, A. Alyamani

**Abstract.** The room temperature laser generation in the yellow – green ( $\lambda = 558.5\text{--}566.7\text{ nm}$ ) spectral range has been demonstrated under optical pumping by a pulsed nitrogen laser of Cd(Zn)Se/ZnSe quantum dot heterostructures. The maximum achieved laser wavelength was as high as  $\lambda = 566.7\text{ nm}$  at a laser cavity length of  $945\text{ }\mu\text{m}$ . High values of both the output pulsed power (up to  $50\text{ W}$ ) and the external differential quantum efficiency ( $\sim 60\%$ ) were obtained at a cavity length of  $435\text{ }\mu\text{m}$ . Both a high quality of the laser heterostructure and a low lasing threshold ( $\sim 2\text{ kW cm}^{-2}$ ) make it possible to use a pulsed InGaN laser diode as a pump source. A laser microchip converter based on this heterostructure has demonstrated a maximum output pulse power of  $\sim 90\text{ mW}$  at  $\lambda = 560\text{ nm}$ . The microchip converter was placed in a standard TO-18 ( $5.6\text{ mm}$  in diameter) laser diode package.

**Keywords:** semiconductor lasers, laser converter, optical pumping, yellow–green lasing.

## 1. Introduction

Interest to the development of compact lasers emitting in the yellow–green spectral region ( $\lambda = 558.5\text{--}566.7\text{ nm}$ ) is caused by their applicability in biology, medicine, and optical communications, as well as in multimedia laser projectors for extending the colour space. At present, the maximum wavelength of commercial InGaN/GaN laser diodes (LDs) operating in the cw regime is  $\sim 520\text{ nm}$  at room temperature [1, 2]. Unfortunately, stimulated yellow–green emission in nitride-based semiconductor structures is difficult to obtain due to a rather high lasing threshold and a low reliability of these lasers caused by the main problems of formation of low-defect-density InGaN quantum wells with a high indium content, which is necessary to obtain a required emission wavelength [3]. The compact solid-state lasers with frequency dou-

bling pumped by IR LDs could emit in the yellow–green range. However, these lasers have a fixed wavelength, a comparatively low operating speed, and require expensive nonlinear crystals to obtain a high conversion efficiency.

An alternative way is the creation of a compact  $A^2B^6/A^3N$  laser converter, in which the Cd(Zn)Se/ZnMgSSe laser nano-heterostructure is pumped by blue-violet radiation of an InGaN LD. Previously, we showed the possibility of creating low-threshold highly efficient optically pumped lasers based on Cd(Zn)Se/ZnMgSSe heterostructures with the active region consisting of one or several planes of self-assembled Cd(Zn)Se/ZnSe quantum dots (QDs) in a graded-index waveguide [4, 5], as well as the possibility of creating  $A^2B^6/A^3N$  converters based on these lasers for the green ( $\lambda = 520\text{--}550\text{ nm}$ ) spectral region [6, 7]. The possibility of industrial production of active elements for this converter, as well as a noticeable decrease in the cost of commercial InGaN LDs used in Blu-ray discs ( $\lambda \sim 405\text{ nm}$ ) and DPL projectors ( $\lambda \sim 445\text{ nm}$ ), determine the prospects for the creation of this device. In this work, we present the results of development and production of low-threshold highly efficient Cd(Zn)Se/ZnSe QD lasers emitting in the yellow–green spectral region and of a semiconductor microchip converter based on these lasers.

## 2. Experimental

The (Zn, Mg)(S, Se) structures for optically pumped lasers were grown by molecular-beam epitaxy pseudomorphically on GaAs (001) substrates using a two-chamber SemiTeq STE 3526 (Russia) setup. The structures contain lower and upper ZnMgSSe cladding layers ( $E_g \sim 2.87\text{--}2.93\text{ eV}$  at the temperature  $T = 295\text{ K}$ ) with the thicknesses of  $1.2$  and  $0.02\text{ }\mu\text{m}$ , respectively; an asymmetric graded-index waveguide; and an active region consisting of two electronically coupled layers of self-assembled Cd(Zn)Se/ZnSe QDs with an increased nominal thickness of  $2.9\text{--}3.1$  monolayers ( $0.85\text{--}0.90\text{ nm}$ ), separated by a  $5\text{-nm}$ -thick ZnSe layer. The asymmetric graded-index waveguide with a total thickness of  $0.3\text{--}0.4\text{ }\mu\text{m}$  was composed of a set of  $\text{Zn}_{0.89}\text{Mg}_{0.11}\text{S}_{0.16}\text{Se}_{0.84}/\text{ZnSe}$  and  $\text{ZnS}_{0.15}\text{Se}_{0.85}/\text{ZnSe}$  ( $E_g \sim 2.72\text{--}2.84\text{ eV}$  at  $T = 295\text{ K}$ ) short-period superlattices with variable period and well-to-barrier thickness ratio at fixed magnesium and sulphur contents in the layers. The average lattice parameter of the ZnSSe/ZnSe superlattice closest to the active region was shifted to lower values with respect to the GaAs lattice parameter (by  $400''$  according to the  $\Theta$ - $2\Theta$  X-ray diffraction rocking curve) in order to compensate the strong compressive strain induced by the large nominal thickness of the CdSe QD layers and thus to

E.V. Lutsenko, A.G. Voinilovich, N.V. Rzhetskii, V.N. Pavlovskii, G.P. Yablonskii B.I. Stepanov Institute of Physics, National Academy of Sciences of Belarus, prosp. Nezavisimosti 68, 220072 Minsk, Belarus; e-mail: e.lutsenko@infanbel.bas-net.by;  
S.V. Sorokin, S.V. Gronin, I.V. Sedova, P.S. Kop'ev, S.V. Ivanov A.F. Ioffe Physical-Technical Institute, ul. Politekhnicheskaya 26, 194021 St. Petersburg, Russia; e-mail: irina@beam.ioffe.rssi.ru;  
M. Alanzi, A. Hamidalddin, A. Alyamani KACST, National Nanotechnology Center, P.O. BOX 6086 Riyadh – 11442, Saudi Arabia; e-mail: ayamani@kacst.edu.sa

Received 27 February 2013

Kvantovaya Elektronika 43 (5) 418–422 (2013)

Translated by M.N. Basieva

maintain the coherence of the structure. Optimisation of the initial stage of the ZnSe/GaAs heterointerface formation according to the procedure described in [5] allowed us to achieve better structural perfection of laser heterostructures and to decrease the stacking fault density down to  $10^5 \text{ cm}^{-2}$ , which is evidenced by the structure surface microphotograph obtained using a fluorescent microscope (Fig. 1). The dark point is a stacking fault. The weak modulation of the emission intensity in the photograph is probably related to an inhomogeneous distribution of emitting QDs, which localise nonequilibrium carriers, over the active region.

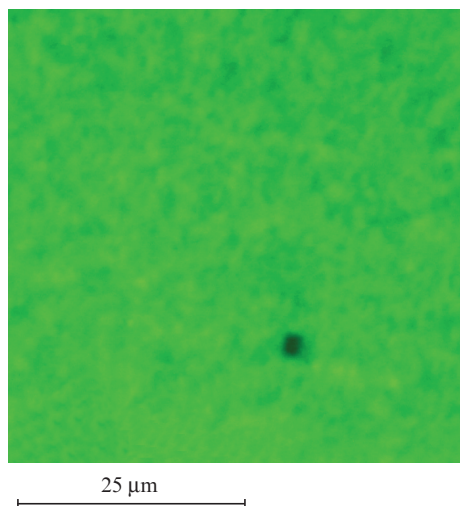


**Figure 1.** Microphotograph of the laser heterostructure surface obtained using a fluorescent microscope.

Optical pumping of cleaved cavity structures was performed by radiation of a nitrogen laser ( $\lambda = 337 \text{ nm}$ ,  $f = 1 \text{ kHz}$ ,  $\tau = 10 \text{ ns}$ ) focused into a strip  $200 \mu\text{m}$  wide in the transverse geometry at room temperature. The converter was created using a commercial pulsed InGaN LD with a nominal power of  $1 \text{ W}$  ( $\lambda = 437 \text{ nm}$ ,  $f = 1 \text{ kHz}$ ,  $\tau = 200 \text{ ns}$ ).

### 3. Results and discussion

#### 3.1. Optical pumping of heterostructures by a $\text{N}_2$ laser pulse

Laser emission in the heterostructure under study was obtained under transverse optical pumping of samples with different cavity lengths by a pulsed  $\text{N}_2$  laser at room temperature. With increasing the cavity length from  $\sim 150$  to  $\sim 1000 \mu\text{m}$ , the emission wavelength increased from  $558.5$  to  $566.7 \text{ nm}$ , which was caused by a long-wavelength shift of the gain peak with decreasing lasing threshold from  $\sim 4$  to  $\sim 2 \text{ kW cm}^{-2}$ . The above wavelengths correspond to the yellow–green spectral region.

Figure 2 shows the spectra of radiation emitted from the edge of the laser with a cavity length of  $945 \mu\text{m}$  at the temperature  $T = 295 \text{ K}$  and the integral intensity of this radiation as a function of the pump radiation intensity  $I_p$ . One can see a narrow laser peak with  $\lambda = 566.7 \text{ nm}$  superimposed on the wide photoluminescence band at  $I_p \sim 2.2 \text{ kW cm}^{-2}$ . The directivity diagram of the TE-polarised laser radiation contains one lobe with a maximum directed along the cavity axis

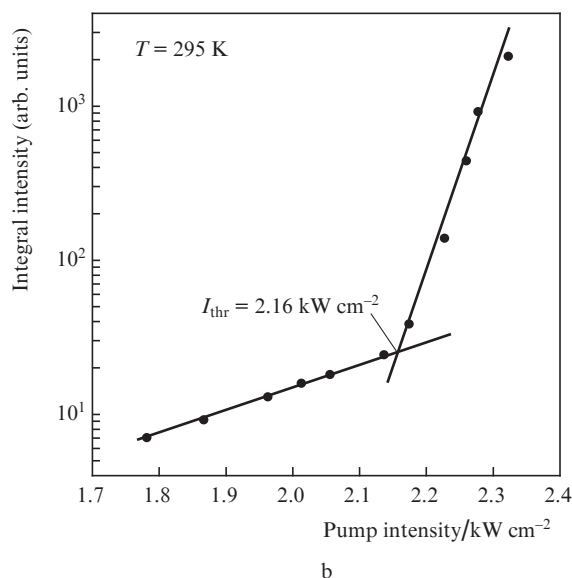
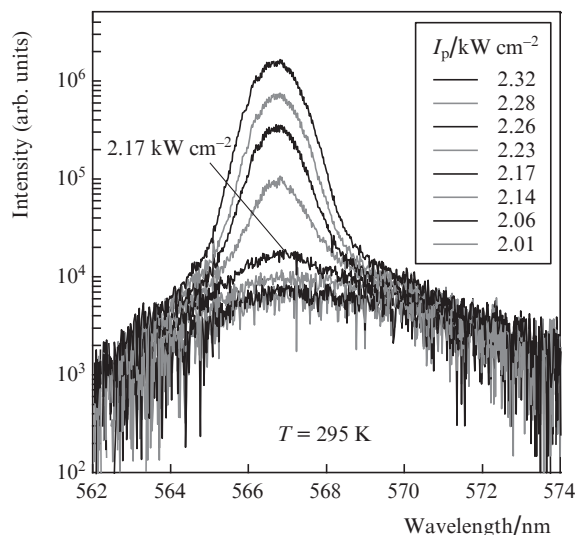


**Figure 2.** Emission spectra of the laser with the cavity length  $945 \mu\text{m}$  recorded from the laser face at different pump intensities  $I_p$  (a) and integral intensity of this radiation as a function of the pump intensity (b).

and with a width at half-maximum of  $30^\circ$ , which corresponds to the generation on the fundamental mode of the optical waveguide. The lasing threshold determined from the dependence of the integral emission intensity on the pump intensity was as low as  $2.16 \text{ kW cm}^{-2}$  (Fig. 2b).

Figure 3 shows the dependence of the output power of a laser with a cavity length of  $435 \mu\text{m}$  on the pulsed pump power. As is seen, the output power linearly increases with increasing pump power and reaches a maximum of  $\sim 50 \text{ W}$ . The external differential efficiency  $\eta$  is  $\sim 28\%$ , which corresponds to the external differential quantum efficiency  $\eta_d^Q \sim 59\%$ . However, with a further increase in the pump power, the laser power sharply decreases and the laser wavelength shifts to the blue by more than  $2 \text{ nm}$ . In this case, the far-field pattern in the plane of the heterostructure becomes strongly inhomogeneous and considerably smears, while the lasing threshold irreversibly increases and the laser efficiency decreases.

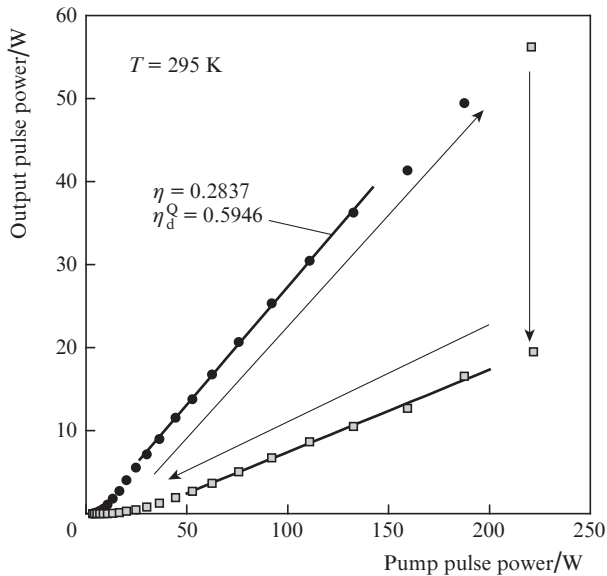


**Figure 3.** Dependence of the output pulse power of the laser with a cavity length of 435  $\mu\text{m}$  on the pump pulse power. Squares show the power during and after degradation.

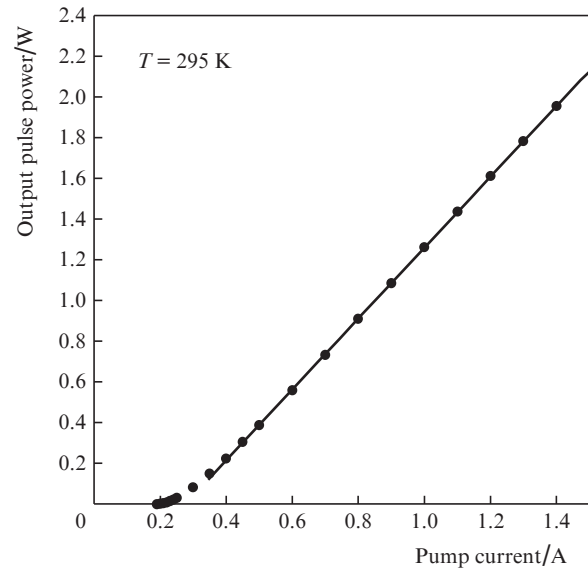


**Figure 4.** Power–current characteristic of the InGaN LD pumped by 200-ns current pulses with a repetition rate of 300 Hz.

This catastrophic optical degradation occurring under action of the generated laser radiation was previously observed in similar structures [8] and is caused by the destruction of the heterostructure regions adjacent to the cavity mirrors. It should be noted that the catastrophic degradation threshold in the studied structure is higher than in green-emitting structures with non-optimised structural quality, in which degradation occurred even at the output power of 12–13 W from one cavity face at the same width of the excitation strip. The higher degradation resistance of the studied lasers is explained by a low stacking defect density in the structures (Fig. 1) and by a high structural perfection of the grown heterostructure, which was achieved due to the compensation of mechanical stresses in the structure and to the optimisation of the initial heteroepitaxy stage according to [5].

Thus, the created lasers emitting in the yellow–green spectral region are highly competitive in characteristics with the best green lasers based on Cd(Zn)Se/ZnSe QD heterostructures and are promising for creating microchip converters.

### 3.2. Microchip converter

To create a converter, we used a commercial InGaN LD emitting at  $\lambda = 437$  nm. Figure 4 shows the power–current characteristic of this LD pumped by 200-ns current pulses. As is seen, lasing starts at a current of  $\sim 0.2$  A. The differential efficiency determined from the slope of the linear part of the power–current characteristic was 1.74 W/A. The LD output power at the maximum pump current was 1.96 W.

Based on this InGaN LD, we designed a microchip converter and obtained yellow–green radiation of a converter at room temperature for the first time. To create a microchip converter, the InGaN LD radiation was focused by a cylindrical microlens into a narrow strip oriented perpendicular to the cleaves of the Cd(Zn)Se/ZnMgSSe laser heterostructure. The cavity length of the Cd(Zn)Se/ZnMgSSe laser ( $L_{\text{cav}} = 114$   $\mu\text{m}$ ) and the microlens dimensions were chosen to obtain

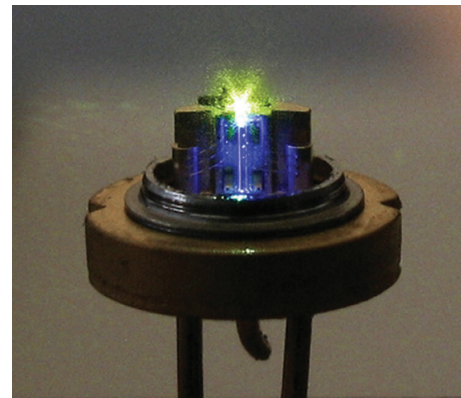


**Figure 5.** Photograph of the microchip converter under operating conditions.

the minimum size of the device and the minimum threshold pump power [9]. A photograph of the microchip converter under operating conditions is given in Fig. 5. One can see that the developed integral construction is entirely placed in a standard TO-18 LD package (diameter 5.6 mm).

Figure 6a shows the microchip converter emission spectra at different pump currents of the InGaN LD. At a current higher than 710 mA, on the background of the wide spectral envelope of amplified photoluminescence, one can see a narrow laser band, which corresponds to a sharp increase in the integral intensity of radiation (Fig. 6b). The laser line maximum corresponds to the wavelength  $\lambda = 560$  nm. The mode structure of the laser spectrum is determined by the longitudinal modes of the Fabry–Perot resonator formed by the plane-parallel cleaves of the heterostructure.

Figure 7 presents the dependence of the microchip converter output power on the current through the InGaN LD. It is seen that, at a current exceeding 1 A, the converter output power linearly increases with increasing current through the diode. At the maximum pump current of 1.4 A, the output

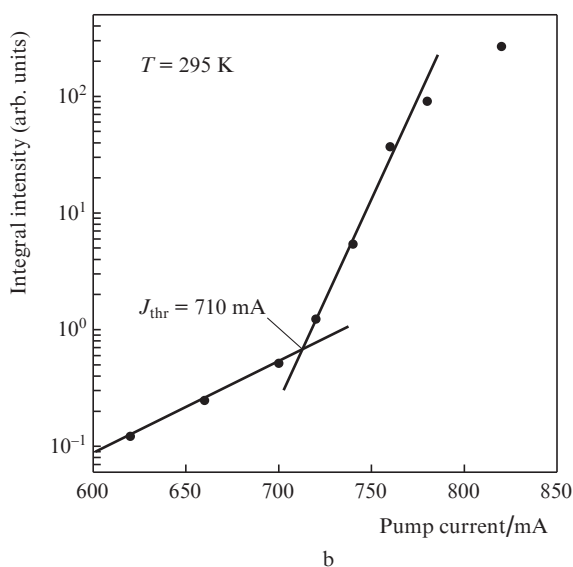
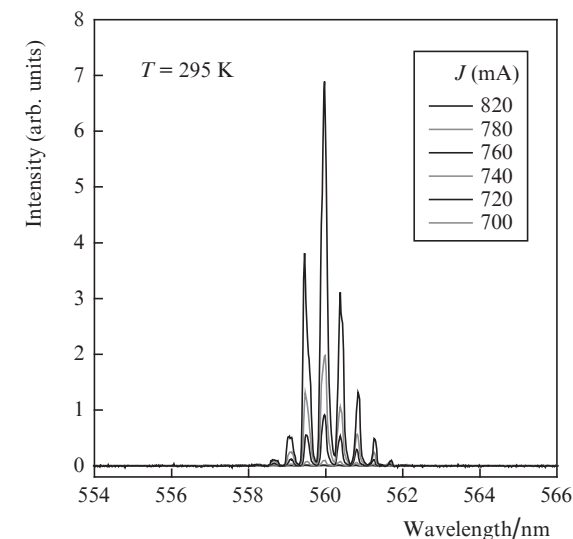


**Figure 6.** Emission spectra of the microchip converter at different pump currents  $J$  (decreases from the top to the bottom) of the InGaN LD (a) and dependence of the integral intensity of this radiation on the pump current (b).

power reaches 89 mW, which corresponds to the blue-to-yellow-green conversion efficiency of  $\sim 4.5\%$ . The low converter efficiency (compared to the efficiency in the case of pumping by a nitrogen laser) is caused first all by the fact that the pump intensity in the case of LD pumping only slightly exceeds the lasing threshold of the ZnSe heterostructure. The converter efficiency can be considerably increased by decreasing the excited strip width and improving its homogeneity by optimising the LD beam focusing and using specially designed broadband LDs with increased output power.

In addition, an increase in the converter efficiency can be achieved by deposition of antireflection coating on the working surface and a highly-reflecting coating on one of the output faces of the Cd(Zn)Se/ZnMgSSe laser, as well as by optimisation of the heterostructure design for a given wavelength of the pumping LD. Thus, it is expected that the microchip

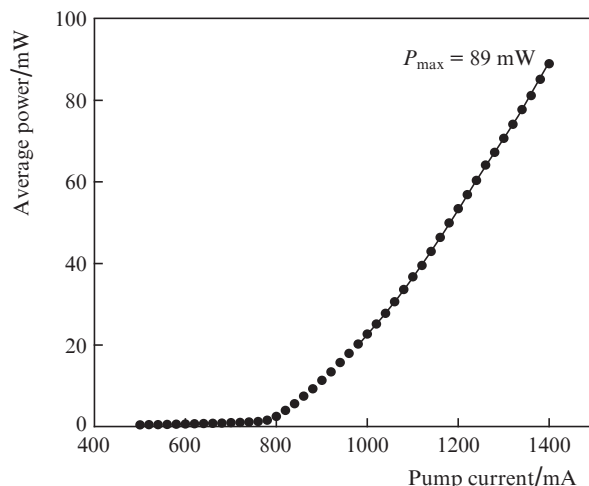


**Figure 7.** Dependence of the microchip converter output power on the InGaN LD pump power.

laser efficiency and power will be considerably increased in the future.

## 4. Conclusions

We obtained low-threshold ( $\sim 2 \text{ kW cm}^{-2}$ ) laser emission in the yellow-green spectral region ( $\lambda = 558.5\text{--}566.7 \text{ nm}$ ) under optical excitation of heterostructures with an active region based on two electronically coupled layers of self-assembled Cd(Zn)Se/ZnSe QDs and with a graded-index superlattice waveguide, which were grown by molecular-beam epitaxy on GaAs (001) substrates. Based on these heterostructures, a compact semiconductor microchip laser ( $\lambda = 560 \text{ nm}$ ) with a maximum pulsed power of  $\sim 90 \text{ mW}$  is created for the first time. The laser microchip converter is a chip assembly consisting of a Cd(Zn)Se/ZnMgSSe heterostructure ( $L_{\text{cav}} = 114 \mu\text{m}$ ) pumped by a violet InGaN LD beam focused by a cylindrical microlens. The entire microchip laser is placed in a standard (5.6 mm in diameter) laser diode package.

## References

1. Nichia Green Laser Diode NDG4216 datasheet (2012); <http://www.nichia.co.jp/specification/en/product/ld/NDG4216-E.pdf>.
2. Osram Opto Semiconductors. Green Single Mode Lasers in TO Package (2012); <http://catalog.osram-os.com/>.
3. Avramescu A., Lerner T., Möller J., Eichler C., Bruederl G., Sabathil M., Lutgen S., Strauss U. *Appl. Phys. Express*, **3**, 061003 (2010); Takagi S., Enya Y., Kyono T., Adachi M., Yoshizumi Y., Sumitomo T., Yamanaka Y., Kumano T., Tokuyama S., Sumiyoshi K., Saga N., Ueno M., Katayama K., Ikegami T., Nakamura T., Yanashima K., Nakajima H., Tasai K., Naganuma K., Fuutagawa N., Takiguchi Y., Hamaguchi T., Ikeda M. *Appl. Phys. Express*, **5**, 082102 (2012).
4. Sedova I.V., Lutsenko E.V., Gronin S.V., Sorokin S.V., Vainilovich A.G., Sitnikova A.A., Yablonskii G.P., Alyamani A., Fedorov D.L., Kop'ev P.S., Ivanov S.V. *Appl. Phys. Lett.*, **98**, 171103 (2011).
5. Gronin S.V., Sedova I.V., Sorokin S.V., Klimko G.V., Belyaev K.G., Lebedev A.V., Sitnikova A.A., Toropov A.A., Ivanov S.V. *Phys. Status Solidi C*, **9**, 1833 (2012).

6. Lutsenko E.V., Vainilovich A.G., Tarasuk N.P., Pavlovskii V.N., Yablonskii G.P., Alyamani A., Sedova I.V., Sorokin S.V., Gronin S.V., Kop'ev P.S., Ivanov S.V. *Phys. Status Solidi C*, **9**, 1837 (2012).
7. Sorokin S.V., Sedova I.V., Gronin S.V., Klimko G.V., Belyaev K.G., Ivanov S.V., Alyamani A., Lutsenko E.V., Vainilovich A.G., Yablonskii G.P. *Electron. Lett.*, **48**, 118 (2012).
8. Zubelevich V.Z., Voinilovich A.G., Lutsenko E.V., Yablonskii G.P., Shulenkov A.S., Sorokin S.V., Sedova I.V., Gronin S.V., Ivanov S.V., Kalisch H., Heuken M. *Trudy konf. 'Poluprovodnikovye lasery i sistemy'* (Proc. Conf. 'Semiconductor Lasers and Systems') (Minsk, 2011) p. 123.
9. Lutsenko E.V., Sorokin S.V., Sedova I.V., Vainilovich A.G., Tarasuk N.P., Pavlovskii V.N., Yablonskii G.P., Gronin S.V., Kop'ev P.S., Ivanov S.V. *Phys. Status Solidi B*, **247**, 1557 (2010).